# The Risk of Being Killed by Earthquakes in Melbourne: A Preliminary Study

**Hing-Ho Tsang[1]*, James E. Daniell[2], Friedemann Wenzel[2], John L. Wilson[1]**

1. Swinburne University of Technology, Melbourne, Australia
   * Email: htsang@swin.edu.au (Corresponding Author)

2. Karlsruhe Institute of Technology, Karlsruhe, Germany

## Abstract

Even our structures have been designed strictly in accordance to the required code of practice, fatalities are still unavoidable in extreme earthquakes. This is the residual risk, which should be minimised to an acceptable level. Hence, it is essential to estimate the potential earthquake fatalities for informed policy making. In this study, the probable maximum loss (PML) of life in the Greater Melbourne Region will be estimated using SELENA software for a suite of earthquake scenarios as a function of the associated return period. Such a PML curve for fatalities is called an *F-N* curve, which characterises the annual rate (or frequency), *F*, of exceeding *N* fatalities.

**Keywords:** Societal risk; *F-N* curve; Recurrence relationship; Fatality; Loss; Earthquake

## 1 Introduction

Societal risk was defined by Jones (1992) as "the relationship between frequency and the number of people suffering from a specified level of harm in a given population from the realisation of specified hazards." As a damaging earthquake can lead to widespread destruction and casualties, in the scale of a city or a province, the societal risk should then be quantified for a region. Also, it is desirable if the societal risk is evaluated in a probabilistic manner, from which the outcome would be a recurrence relationship for an event-based loss quantity, economic loss or casualty, i.e. frequency-number (*F-N*) curve if fatality is the loss quantify being evaluated.

Earthquake loss estimation is an important tool, which is commonly used for quantifying the probable risk to a single asset, such as a building, a critical facility or a lifeline infrastructure The outcome is used by its owner, asset manager and re-insurance corporation for decision making regarding the need of retrofitting or sharing of risk through financial tools. The assessment can be extended for the estimation of individual fatality risk, which can be used as another governing parameter for risk-based seismic design or safety evaluation (e.g. Tsang and Wenzel 2016).

Regional earthquake loss modelling is typically conducted by government agencies, re-insurance sector or asset managers of spatially distributed infrastructure for assessing the resiliency of a city, evaluating probable financial impact, or deriving disaster management plan. It is usually done for selected scenario earthquakes, each of which may be associated with a return period, such that the outcomes carry some meanings of the probability of occurrence. Alternatively, a fully stochastic approach can be adopted. The outcome can be used for evaluating the overall earthquake safety of society at different scale: precinct, city, state/province or country (e.g. Tsang et al. 2018a).

This paper presents the estimates of earthquake fatalities through a simple and transparent semi-probabilistic procedure (proposed in Tsang et al. 2018b) based on risk modelling of earthquake scenarios that are consistent with a wide range of the probabilistic hazard. The proposed approach retains the essential details that have more significant influence to the outputs, whilst simplifications are made to the relatively less important aspects. Societal risk recurrence function, or an *F-N* curve, can then be conveniently developed from an existing seismic hazard curve. A parameterisation scheme will also be presented, such that the median societal risk function, or *F-N* curve, and its parameters can be compared between regions in a more systematic way in the future. The semi-probabilistic procedure is illustrated in the rest of the paper using the Greater Melbourne Region as a case study (based on Tsang et al. 2018b).

The procedure for developing societal risk function involves the key following steps:
Step 1: Definition and characterisation of the study region
Step 2: Selection of response-specific probabilistic scenarios
Step 3: Scenario-based loss modelling
Step 4: Construction of societal risk function

## 2 Characterisation of the Greater Melbourne Region

Melbourne (Coordinates: 37°48’49” S, 144°57’47” E) has a total population of 4,205,584 (as of 2011) according to the Australian Bureau of Statistics. In this case study, the whole region is divided into 9,658 geo-units, as defined by the Australian Statistical Geography Standard (ASGS 2016) based on the census data of 2011, and can be found in the National Exposure Information System (NEXIS) developed by Geoscience Australia. The population density of each geo-unit are shown in Fig. 1.

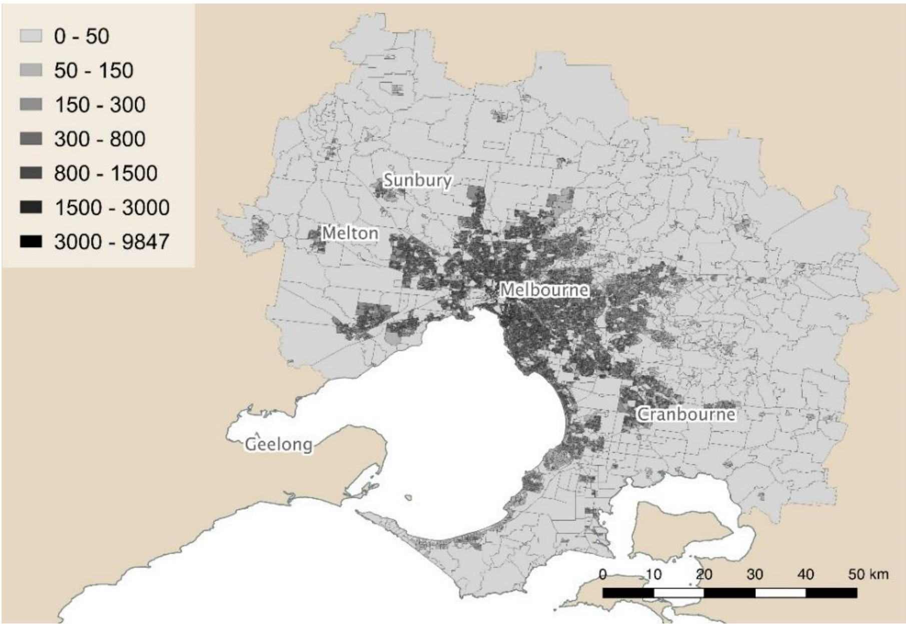


**Fig. 1** Population density in each of the 9,658 geo-units in the Greater Melbourne Region (in the unit of the number of people per square metre times $10^{-5}$) (Tsang et al. 2018b)

The ground condition of each geo-unit has been broadly categorised according to NEHRP soil classification scheme, based on the average shear wave velocity over the upper 30 m of sediments inferred from the topographical condition (USGS 2015). Fig. 2 shows the micro-zonation map for the Greater Melbourne Region. By comparing Fig. 2 with Fig. 1, it is clear that the majority of the population is residing in housings that are sitting on either soft rock or dense/stiff soil.

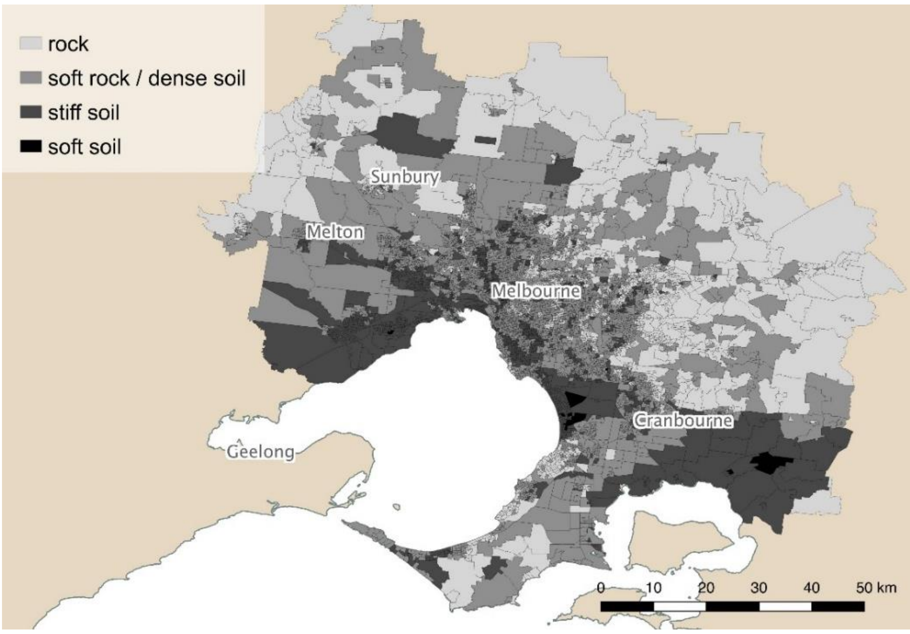


**Fig. 2** Soil class of each of the 9,658 geo-units in the Greater Melbourne Region, categorised according to NEHRP soil classification scheme (Tsang et al. 2018b)

Building exposure data was collected from NEXIS. Table 1 summarises the percentage of population residing in each model building type in the Greater Melbourne Region, based on the classification scheme recommended in HAZUS Technical Manual (2012). The distributions of the ratio (in percent) of floor area of low-rise unreinforced masonry (URML) to the land area of each of the 9,658 geo-units in the Greater Melbourne Region are shown in Fig. 3. The distribution of population (in percent) at different time of a day is based on the recommendation in the User and Technical Manual of SELENA (Molina et al. 2010).

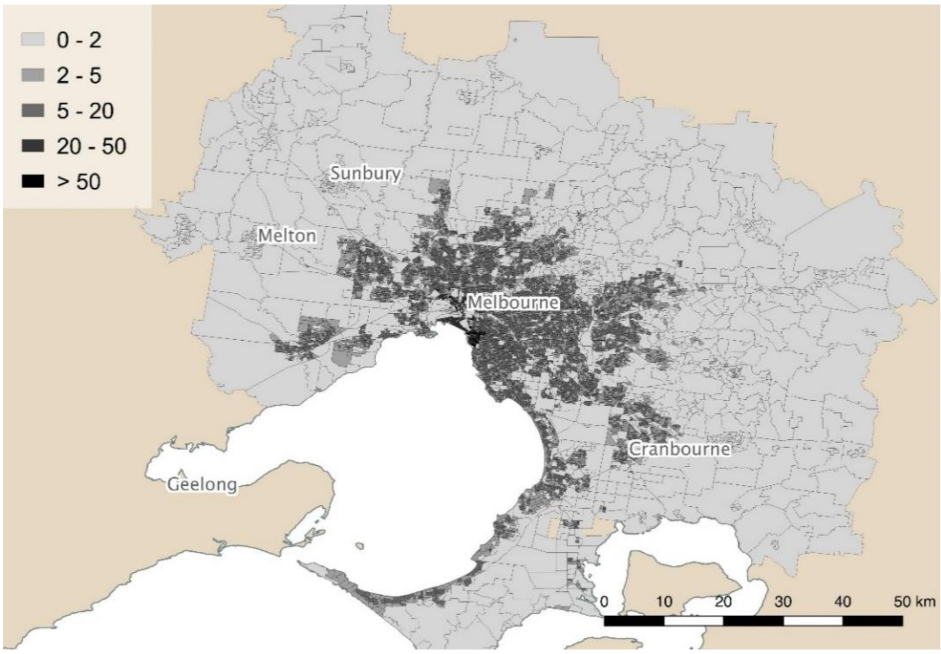


**Fig. 3** Distribution of the ratio (in percent) of floor area of low-rise unreinforced masonry (URML) to the land area of each of the 9,658 geo-units in the Greater Melbourne Region (Tsang et al. 2018b)

**Table 1** Percentage of population residing in each model building type in the Greater Melbourne Region, based on the classification scheme recommended in HAZUS (2012)

| No. | Abbreviation | Description | Percentage |
|---|---|---|---|
| **1** | S1L | Steel moment frame – low-rise (1-3 storeys) | 3.1 |
| **2** | S1M | Steel moment frame – mid-rise (4-7 storeys) | 2.3 |
| **3** | S1H | Steel moment frame – high-rise (8+ storeys) | 0.15 |
| **4** | S4L | Steel frame with cast-in-place concrete shear walls – low-rise (1-3 storeys) | 1.4 |
| **5** | S5L | Steel frame with unreinforced masonry infill walls – low-rise (1-3 storeys) | 3.3 |
| **6** | S5M | Steel frame with unreinforced masonry infill walls – mid-rise (4-7 storeys) | 1.9 |
| **7** | C3L | Concrete frame with unreinforced masonry infill walls – low-rise (1-3 storeys) | 1.4 |
| **8** | C3M | Concrete frame with unreinforced masonry infill walls – mid-rise (4-7 storeys) | 2.5 |
| **9** | PC2M | Pre-cast concrete frames with concrete shear walls – mid-rise (4-7 storeys) | 0 |
| **10** | RM1L | Reinforced masonry bearing walls with wood or metal deck diaphragms – low-rise (1-3 storeys) | 0.41 |
| **11** | RM1M | Reinforced masonry bearing walls with wood or metal deck diaphragms – mid-rise (4-7 storeys) | 0.03 |
| **12** | RM2L | Reinforced masonry bearing walls with pre-cast concrete diaphragms – low-rise (1-3 storeys) | 0.06 |
| **13** | RM2M | Reinforced masonry bearing walls with pre-cast concrete diaphragms – mid-rise (4-7 storeys) | 0.05 |
| **14** | MH | Mobile homes | 0.49 |
| **15** | W1 | Wood, light frame | 56.9 |
| **16** | C1L | Concrete moment frame – low-rise (1-3 storeys) | 5.9 |
| **17** | C1M | Concrete moment frame – mid-rise (4-7 storeys) | 3.6 |
| **18** | C1H | Concrete moment frame – high-rise (8+ storeys) | 0.96 |
| **19** | URML | Unreinforced masonry bearing walls – low-rise (1-3 storeys) | 15.6 |

## 3 Selection of Probabilistic Earthquake Scenarios

It is reasonably expected that the more vulnerable building types across the whole Australia generally is low-rise unreinforced masonry (URML) and low-rise concrete moment frame (C1L), whilst the seismic demand on high-rise buildings is low, which is typical in regions of low-to-moderate seismicity. As the predominant period of these two types of potentially vulnerable constructions is in the order of 0.3 sec, the spectral acceleration response at this single natural period (i.e. $SA_{0.3}$) was adopted for selecting hazard-consistent scenario earthquakes.

PSHA studies were conducted for the study region by various groups, e.g. Geoscience Australia (2012), Schaefer et al. (2015) and Lam et al. (2016). As seismic hazard predictions for annual frequency of exceedance as low as $10^{-5}$ are required for capturing the low-probability but high-loss events, the only set of hazard results that provides estimates for annual frequencies down to $2 \times 10^{-5}$ (i.e. return period of 50,000 years) for Melbourne, Australia, can be found in the study of Somerville et al. (2013), and was therefore adopted in this study. Hence, the uniform hazard spectra (UHS) for different return periods presented in Somerville et al. (2013) were digitised, and the values at 0.3 sec, in the unit of g, were then fitted with a power function. The hazard function in terms of the rate of exceedance, $H$, of $SA_{0.3}$ for rock sites can be represented by Eq. (1):

$$H(SA_{0.3}) = 0.0004 \times \left(\frac{0.34}{SA_{0.3}}\right)^{3.05} \tag{1}$$

in which, $H_0$ = 0.0004 is the reference rate of exceedance, that is corresponding to the common anchoring return period of 2,500 years, for which the value of $SA_{0.3}$ is 0.34g. This is considered applicable across the whole study region, and hence, representing the hazard at the centroid of population. As a spectral amplitude-recurrence relationship based on median ground motion predictions is not available for the study region, a correction factor, $f_{corr}$, of 0.313 is needed for reducing the probabilistic hazard rate (refer Tsang et al. 2018b for details).

Information about the locations and geometry of faults are available from the website of Geoscience Australia (2017). The common faulting mechanism in Australia is reverse faulting due to the compressive behaviour of the continent (Leonard et al. 2002). The major known faults in and surrounding the Greater Melbourne Region are shown in Fig. 4. It is noteworthy that no major fault has been identified in the CBD area and inner suburbs of Melbourne. Table 2 summarises the strike angle (in degree) and length of each major known fault, from which the maximum magnitude considered were estimated based on the correlation in Wells and Coppersmith (1994).

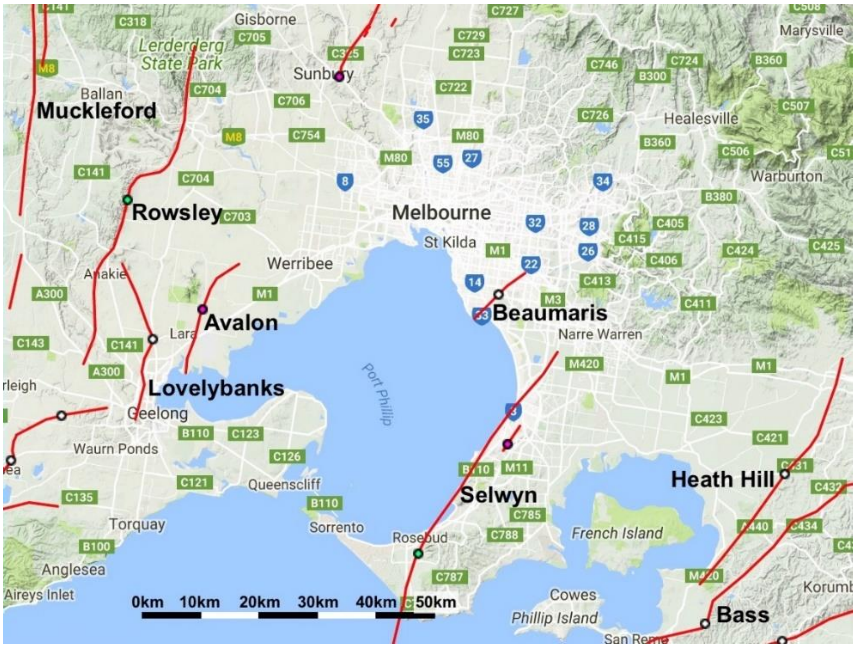


**Fig. 4** Major known faults in and surrounding the Greater Melbourne Region (reproduced from Geoscience Australia 2017 based on Google Maps) (Tsang et al. 2018b)

The probabilistic hazard rate, $H$, in Eq. (1) was then multiplied by the correction factor of 0.313 before the values of spectral response were used for identifying scenario earthquake events. The two major GMPEs employed in the PSHA study by Somerville et al. (2013), i.e. Somerville et al. (2009) and Allen (2012), were used for back-calculating the magnitudes of the response-specific scenarios for each fault along with its distance from the population centroid. 68 scenario earthquakes specifically matched for spectral acceleration response at $T$ = 0.3 sec have been identified and the distribution of the epicentres is shown in Fig. 5.

**Table 2** Maximum magnitude considered for each major known fault, estimated based on the correlation with fault length as proposed by Wells and Coppersmith (1994)

| Name of Fault | Strike Angle (degree) | Length of Fault (km) | Estimated Maximum Magnitude |
|---|---|---|---|
| **Avalon** | 20 | 23.4 | 6.7 |
| **Bass** | 55 | 57.6 | 7.3 |
| **Beaumaris** | 228 | 12.7 | 6.3 |
| **Heath Hill** | 36 | 50.3 | 7.2 |
| **Lovelybanks** | 179 | 31.1 | 6.9 |
| **Muckleford** | 3 | 123 | 7.9 |
| **Rowsley** | 20 | 66 | 7.4 |
| **Selwyn** | 212 | 97 | 7.7 |

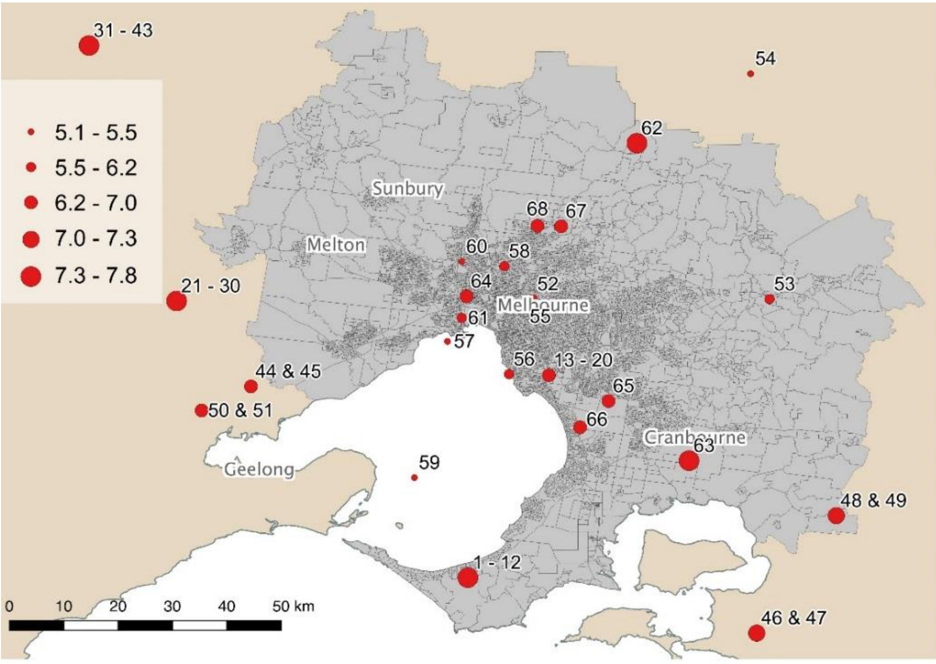


**Fig. 5** Distribution of the epicentres of 68 response-specific probabilistic scenario earthquakes identified for fatality estimation in the Greater Melbourne Region. The size of each circle indicates the relative size (magnitude) of earthquake (Tsang et al. 2018b)

Most of the epicentres are set in the middle of major known faults (Numbers 1 to 51). 17 earthquakes (Numbers 52 to 68) are distributed randomly in the Greater Melbourne Region, amongst which, 7 scenarios (Numbers 62 - 68) are taken from a recent study conducted by Daniell et al. (2015), whilst the others are distributed randomly within a circle of 100 km radius measured from the CBD area.

The strike angle, the dip angle and the fault mechanism for scenario Numbers 1 to 51 are taken from the website of Geoscience Australia (2017). For random event Numbers 52 to 61, the strike angle is assumed as 45 degree, and the dip angle is assumed equal to the average of the dips of faults around the study region, i.e. 50 degree (Clark and Leonard 2014), whilst these values for scenario Numbers 62 to 68 were adopted from the hazard study of Schäfer et al. (2015). The focal depth of earthquake Numbers 1 to 61 is set at 15 km, and the values for earthquake Numbers 62 to 68 were adopted from Daniell et al. (2015) and Schäfer et al. (2015).

## 4 Scenario-based Fatality Estimation

In this study, only fatalities directly due to structural damage are considered, which include both indoor and outdoor fatalities. The latter could be caused by the failure of parapet walls or the fall of non-structural wall panels. However, the estimates exclude those caused by co-existing events like fires, tsunami and landslides, or indirect causes including heart attacks, power failure and the release of hazardous materials.

The computer software SELENA has been adopted for earthquake loss modelling in this case study. The key feature of SELENA compared to other loss estimation software is that a logic tree computational algorithm is implemented, such that epistemic uncertainties of any input (e.g. GMPEs) can be taken into account. Each of the input data is assigned with a factor that defines the relative weighting of the respective branch of the logic tree.

On the other hand, a finite rupture model with a rupture surface geometry has to be defined for each earthquake scenario, along with the selected GMPE(s). A deterministic set of ground motion field can be computed for the study region, whilst spatial correlation of the ground motions can be incorporated as an add-on for a more accurate representation of the uncertainties of the ground motions. A geo-unit is the basic unit in the loss modelling. In other words, the ground motion intensity and the associated response spectral parameters are uniform across the whole unit.

The first seismic structural design code in Australia was introduced in 1979, whilst earthquake-resistant design was basically not exercised until the 1989 Newcastle Earthquake. The Australian Standard for earthquake action was then revised in 1993, and enforced in 1995. However it was not mandated and required for all commercial buildings until around 2008, following the 2007 release of the Australian Standard on earthquake actions, AS 1170.4 (Wilson et al. 2008), as discussed in Menegon et al. (2018). Considering the replacement rate around 2% per year nationally, the majority of the building stock in Australia was not specifically designed for earthquake resistance.

However, this does not necessarily mean that Australian buildings could not sustain the level of earthquake actions that have been stipulated in AS 1170.4, given that the potential seismic performance of a structure is also dependent on soil conditions, building height and structural form. The design wind load can be more significant than the stipulated seismic actions in many cases, which is a common situation amongst regions of low-to-moderate seismicity.

As the structural response behaviours of Australian buildings are not completely known, the recommendations of capacity curves and fragility functions in HAZUS Technical Manual were adopted in this illustration. In HAZUS, the vulnerability of buildings has to be classified based on design code levels, namely, high, moderate and low, according to the Design Seismic Zones specified in the Uniform Building Code (UBC, 1997) (preceding the IBC). Meanwhile, a fourth level, pre-code, is recommended for buildings which were not designed and built according to a modern seismic code. Hence, Australian buildings were conservatively classified at pre-code level by this definition. Also, the number of fatalities was estimated based on the methodology given in Coburn and Spence (2002). The fatality rate and its distribution due to a magnitude 7.8 event occurring at the Muckleford fault (i.e. Number 43 in Fig. 5) is shown in Fig. 6 (with the epicentre annotated).

Fig. 7 shows the fatality rate as a percentage of the population in each model building type due to a magnitude 7.7 earthquake occurring at the Selwyn fault (i.e. Number 12 in Fig. 5). It is seen that the two most fatal building types are low-rise unreinforced masonry (URML) and low-rise concrete frame (C1L). Both of these two building types show around 4.5% of mortality rate. It is noteworthy that medium-rise and high-rise concrete frame buildings (i.e. C1M and C1H) are much safer than the low-rise counterpart, based upon HAZUS capacity curves and fatality estimates.

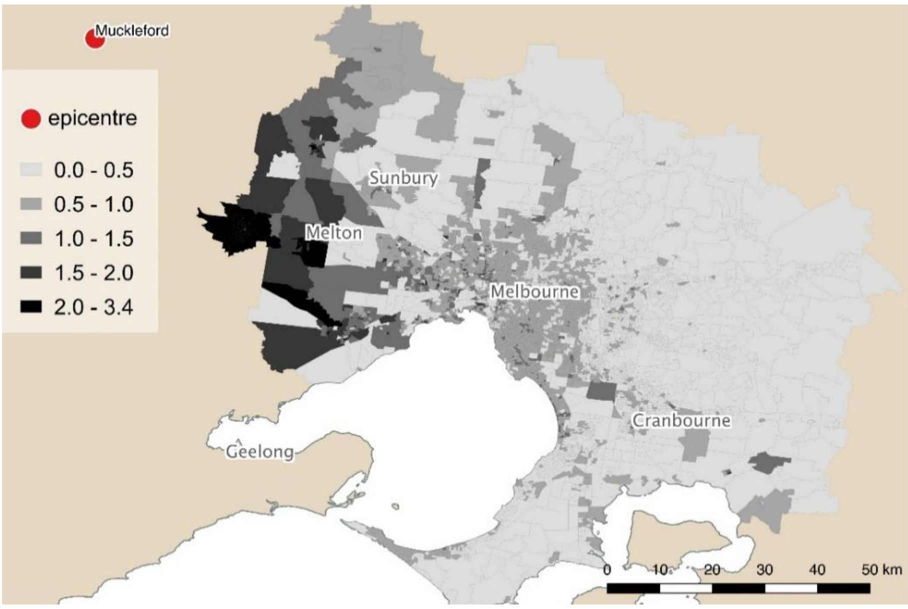


**Fig. 6** Fatality rate as a percentage of the population in each of the 9,658 geo-units in the Greater Melbourne Region due to a magnitude 7.8 earthquake occurring at the Muckleford fault (Tsang et al. 2018b)

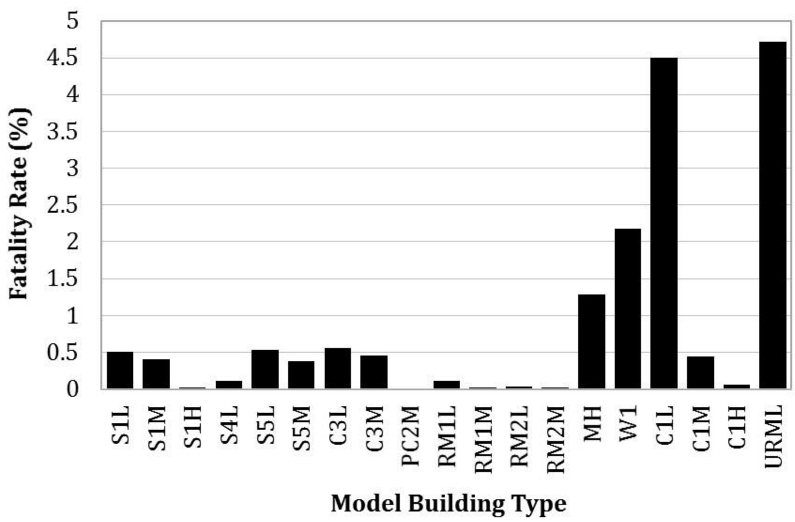


**Fig. 7** Fatality rate as a percentage of the population in each model building type (as defined in Table 1) due to a magnitude 7.7 earthquake occurring at the Selwyn fault

## 5 Parametric *F-N* Function

A societal risk recurrence function, in terms of number of fatalities (i.e. an *F-N* curve), can be constructed based on a dataset of the simulated numbers of fatalities in the Greater Melbourne Region due to a suite of 68 earthquake scenarios as obtained in Section 3, versus the corrected return periods (or frequencies of exceedance) of the hazard. The pairs of values (number of fatalities vs. annual frequency) are plotted in Fig. 8 with both axes in the logarithmic scale.

An upper-truncated Pareto distribution function, Eq. (2), was then calibrated to represent the median properties of the dataset. The reference point of the function, i.e. $N_{ref}$ and $T_{RP,ref}$, is anchored at 2,475 years with 1,800 fatalities. Based on the trend of the dataset at the long return period end, the estimated largest (i.e. truncated) number of fatalities, $N_{max}$, is in the order of 150,000, which is approximately 3.5% of the total population of the region. It is noteworthy that a $b$-value of exactly 1.0 can fit the dataset very well. This translates to a ten times increase in the number of fatalities for every ten times increase in the return period (for the linear portion).

$$\frac{1}{F(N)} = T_{RP}(N) = T_{RP,ref}\left(\frac{{N_{ref}}^{-b} - {N_{max}}^{-b}}{N^{-b} - {N_{max}}^{-b}}\right) = 2{,}475\left(\frac{1{,}800^{-1} - 150{,}000^{-1}}{N^{-1} - 150{,}000^{-1}}\right) \tag{2}$$

If a simplified function is preferred for more convenient communication of risk with a wider group of non-scientific audience, it can be more receptive if the upper truncated part of the *F-N* curve is removed. It will then become the format that is common adopted for setting societal risk criteria in policy and regulation (e.g. Ale 2005).

$$\frac{1}{F} = T_{RP} \cong 2{,}475\left(\frac{N}{1{,}800}\right) = 1.375N \quad \text{for} \quad 1 \leq N \leq 150{,}000 \tag{3}$$

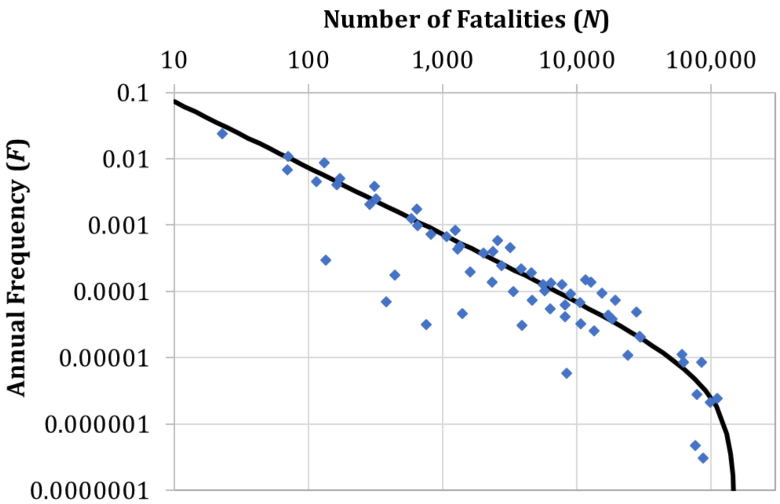


**Fig. 8** Parametric *F-N* curve for the Greater Melbourne Region based on a dataset of the simulated numbers of fatalities (*N*) due to a suite of 68 earthquake scenarios, versus the associated annual frequencies (*F*) of *N* or more fatalities

More case studies need to be conducted in order to examine the generality of such a $b$-value in other parts of the world. A set of $b$-value can be generalised for different types of region and for different loss quantities, then, the key information that is required for deriving a societal risk recurrence function for a region is the reference point only. This can facilitate a systematic analysis and comparison of the societal risk recurrence properties between different regions when such information becomes available in the future.

Furthermore, if the reference point is anchored at a return period typically associated with seismic design or risk assessment, e.g. 475 years or 2,475 years, then, the hazard-consistent scenario earthquakes for a region might have already been identified a priori. The median value of losses can then be estimated based on a suite of representative scenarios with that specific return period. Developing a societal risk function can become more convenient for risk analysts and policy makers.

An Average Annual Loss (*AAL*) of life (or the Potential Loss of Life, *PLL*) can then be estimated using Eq. (4), which results in around 8.5 deaths per year on average. With respect to the population of the study area, this is translated to an average annual mortality rate of 2 in the unit of micromorts (i.e. $2 \times 10^{-6}$), which is a double of the recommended tolerable individual risk limit of 1 micromort (ISO 1998; Tsang and Wenzel 2016). A global view of such mortality rate and the comparison with those of other causes of deaths can be found in Daniell et al. (2017, 2018) and Tsang et al. (2017).

$$AAL \text{ or } PLL \cong \begin{cases} F_{ref} {N_{ref}}^{b} \left( \dfrac{b {N_{max}}^{1-b} - {N_{min}}^{1-b}}{1-b} \right) & \text{for} \quad b \neq 1 \\ F_{ref} N_{ref} \left[ ln \left( \dfrac{N_{max}}{N_{min}} \right) - 1 \right] & \text{for} \quad b = 1 \end{cases} \tag{4}$$

## 6 Conclusions and Closing Remarks

Natural hazard risk is of increasing concern globally, and the associated losses are expected to surge despite immense advances of science and technology. Expected losses due to damage of buildings and infrastructure as well as disruption of economic activities need to be quantified, such that the risk can be properly shared and transferred through various financial tools. Meanwhile, deaths and injuries should be minimised to a level that is tolerable for the society. The reduction and holistic management of risk could then contribute to the socio-economical sustainability internationally.

However, fully probabilistic risk analysis typically requires complex mathematical tools, and the results tend to be meticulously precise but not necessarily accurate or robust. Hence, a direct and easy-to-implement procedure for the analysis of societal earthquake risk is demonstrated in this paper through a case study of the Greater Melbourne Region with number of fatalities as the loss item. It is also recommended that societal risk function can be idealised with a small number of parameters, in order to facilitate region-to-region and hazard-to-hazard comparisons, which may help communicate risk with decision makers and the general public.

## Acknowledgments

The authors gratefully acknowledge the contributions of Ms. Amelie Werner to the results presented in this paper. The financial support from the Bushfire and Natural Hazards Cooperative Research Centre of the Australian Government is also acknowledged.

## References

Ale BJM (2005) Tolerable or acceptable: a comparison of risk regulation in the United Kingdom and in the Netherlands. Risk Analysis 25(2):231–241.

Allen T (2012) Stochastic ground motion prediction equations for southeastern Australian earthquakes using updated source and attenuation parameters. Geoscience Australia Record 2012/69, p. 55.

Clark D, Leonard M (2014) Regional variations in neotectonic fault behaviour in Australia, as they pertain to the seismic hazard in capital cities. In: Proceedings of Australian Earthquake Engineering Society 2014 Conference, Lorne, Victoria, Australia, 21–23 Nov 2014.

Coburn A, Spence R (2002) Earthquake Protection. 2nd Edition, Wiley, 436 pp.

Daniell JE, Schaefer AM, Wenzel F. (2015) A tale of eight cities: earthquake scenario risk assessment for major Australian cities. Proceedings of the 10th Pacific Conference on Earthquake Engineering, Sydney, Australia.

Daniell JE, Schaefer AM, Wenzel F, Tsang HH (2017) The Global Role of Earthquake Fatalities in Decision-Making: Earthquakes versus Other Causes of Fatalities. Proceedings of the Sixteenth World Conference on Earthquake Engineering, Santiago, Chile, January 9-13, 2017.

Daniell, J.E., Pomonis, A., Tsang, H.H., Wenzel, F., Gunasekera, R., Schaefer, A.M. (2018). The Top 100 Fatal Earthquakes: Examining Fatality Risk Reduction Globally with Respect to Seismic Code Implementation. In: Proceedings of the 16th European Conference on Earthquake Engineering, Thessaloniki, Greece, June 18-21, 2018.

FEMA (2012) Hazus®-MH 2.1, Multi-hazard Loss Estimation Methodology – Earthquake Model, Technical Manual. Federal Emergency Management Agency (FEMA), Washington, D.C., U.S.

Geoscience Australia (2012) The 2012 Australian Earthquake Hazard Map. D.R. Burbridge (ed.), Record 2012/71, GeoCat 74811, Geoscience Australia, Canberra, Australia.

Geoscience Australia (2017) Neotectonic Features. Earthquakes@GA.

ISO (1998) ISO 2394:1998. General Principles on Reliability for Structures. International Organization for Standardization (ISO), Geneva.

Jones DA (1992) Nomenclature for hazard and risk assessment in the process industries. Institution of Chemical Engineers (IChemE).

Lam NTK, Tsang HH, Lumantarna E, Wilson JL (2016) Minimum loading requirements for areas of low seismicity. Earthquake and Structures 11(4):539-561.

Leonard M, Ripper ID, Yue L (2002) Australian earthquake fault plane solutions. Geoscience Australia, Department of Industry, Tourism & Resources, Australian Government.

Menegon SJ, Wilson JL, Lam NTK, McBean P (2018) RC Walls in Australia: Seismic Design and Detailing to AS 1170.4 and AS 3600. Australian Journal of Structural Engineering 19(1):67-84.

Molina S, Lang DH, Lindholm CD (2010) SELENA – An open-source tool for seismic risk and loss assessment using a logic tree computation procedure. Computers and Geosciences 36(3):257–269.

Schaefer AM, Daniell JE, Wenzel F (2015) The seismic hazard of Australia – a venture into an uncertain future. Proceedings of the 10th Pacific Conference on Earthquake Engineering, Sydney, Australia, November 6-8, 2015.

Somerville P, Graves R, Collins N, Song SG, Ni S, Cummins P (2009) Source and ground motion models for Australian earthquakes. Proceedings of the 2009 Australian Earthquake Engineering Conference, Newcastle, Australia, December 11-13, 2009.

Somerville P, Bayless J, Skarlatoudis A, Thio HK (2013) Assessment of seismic design motions at low probabilities: comparing Australia and New Zealand. Proceedings of the 2013 Australian Earthquake Engineering Conference, Hobart, Tasmania, Australia, November 15-17, 2013.

Tsang HH, Wenzel F (2016) Setting Structural Safety Requirement for Controlling Earthquake Mortality Risk. Safety Science 86:174-183.

Tsang HH, Wenzel F, Daniell JE (2017) Residual Fatality Risk Estimates for Setting Earthquake Safety Requirement. Proceedings of the Sixteenth World Conference on Earthquake Engineering, Santiago, Chile, January 9-13, 2017.

Tsang, H.H., Daniell, J.E., Wenzel, F. (2018a). Seismic Performance Requirements Based on Individual and Societal Fatality Risk. In: Proceedings of the 16th European Conference on Earthquake Engineering, Thessaloniki, Greece, June 18-21, 2018.

Tsang HH, Daniell JE, Wenzel F, Werner AC. (2018b). A Semi-Probabilistic Procedure for Developing Societal Risk Function. Natural Hazards;92(2):943-969.

Wells DL, Coppersmith KJ (1994) New empirical relationships among magnitude, rupture length, rupture width, rupture area, and surface displacement. Bulletin of the Seismological Society of America 84(4):974–1002.

Wilson JL, Lam NTK, Pham L (2008) Development of the new Australian earthquake loading standard. Special Issue: Earthquake engineering in the low and moderate seismic regions of Southeast Asia and Australia, Electronic Journal of Structural Engineering 8(S1):25–30.